

## Alternating current-dielectrophoresis driven on-chip collection and chaining of green microalgae in freshwaters

Coralie Suscillon,<sup>1</sup> Orlin D. Velev,<sup>2</sup> and Vera I. Slaveykova<sup>1,a)</sup>

<sup>1</sup>*Aquatic Biogeochemistry and Ecotoxicology, Institute F.-A. Forel, Earth and Environmental Science, Faculty of Sciences, University of Geneva, 10, route de Suisse, CH-1290 Versoix, Switzerland*

<sup>2</sup>*Department of Chemical and Biomolecular Engineering, North Carolina State University, Raleigh, North Carolina 27695-7905, USA*

(Received 18 January 2013; accepted 1 April 2013; published online 16 April 2013)

The capability of the AC dielectrophoresis (DEP) for on-chip capture and chaining of microalgae suspended in freshwaters was evaluated. The effects of freshwater composition as well as the electric field voltage, frequency, and duration, on the dielectrophoretic response of microalga *Chlamydomonas reinhardtii* were characterized systematically. Highest efficiency of cell alignment in one-dimensional arrays, determined by the percentage of cells in chain and the chain length, was obtained at AC-field of 20 V mm<sup>-1</sup> and 1 kHz applied for 600 s. The DEP response and cell alignment of *C. reinhardtii* in water sampled from lake, pond, and river, as well as model media were affected by the chemical composition of the media. In the model media, the efficiency of DEP chaining was negatively correlated to the conductivity of the cell suspensions, being higher in suspensions with low conductivity. The cells suspended in freshwaters, however, showed anomalously high chaining at long exposure times. High concentrations of nitrate and dissolved organic matter decrease cell chaining efficiency, while phosphate and citrate concentrations increase it and favor formation of longer chains. Importantly, the application of AC-field had no effect on algal autofluorescence, cell membrane damage, or oxidative stress damages in *C. reinhardtii*. © 2013 AIP Publishing LLC [<http://dx.doi.org/10.1063/1.4801870>]

### I. INTRODUCTION

Microalgae are used as standard organisms in testing the toxicity of various micropollutants as well as common biological components in the whole-cell biosensors and microarrays.<sup>1,2</sup> However, the reproducible immobilization of the living cells for biosensing applications while maintaining their viability is still a major challenge.<sup>3</sup> Recent progress in the field of electrokinetic cell manipulation opens the possibility for rapid on-chip separation, concentration, and immobilization.<sup>4,5</sup> More specifically, dielectrophoresis (DEP) offers means to electrically control the trapping, focusing, translation, or fractionation of particles from mineral, chemical, and biological analytes in a fluid medium, when the right combinations of electrode array designs and electric signals are identified.<sup>6,7</sup>

DEP is defined as a motion of dielectric particles or cells that interact with a non-uniform electric field, which leads to their polarization. DEP mobility is driven by the time-average dielectrophoretic force ( $F_{DEP}$ ), which for a round cell is approximated as<sup>6</sup>

$$F_{DEP} = 2\pi\epsilon_m r^3 \text{Re}[CM(\omega)] \nabla E^2(r), \quad (1)$$

<sup>a)</sup> Author to whom correspondence should be addressed. Electronic mail: vera.slaveykova@unige.ch. Telephone: + 41 22 379 03 35. Fax: + 41 22 379 03 29.

where  $\epsilon_m$  is the permittivity of the surrounding media,  $r$  is the radius of the cell,  $E$  is the electric field intensity, and  $CM(\omega)$  is the Clausius-Mossotti factor, whose real part  $Re[\cdot]$  corresponds to the polarizability function of a bioparticle and depends on the complex permittivity of the medium  $\epsilon_m^*$  and the cell  $\epsilon_{cell}^*$  (Refs. 6 and 8) in the following equation:

$$CM(\omega) = \frac{\epsilon_{cell}^* - \epsilon_m^*}{\epsilon_{cell}^* + 2\epsilon_m^*}. \quad (2)$$

The formation of one dimensional arrays or “pearl-chains” in the direction of the applied electric field involves cell-cell interactions resulting in a chaining force  $F_{chain}$ <sup>6,8–11</sup>

$$F_{chain} = -C\pi\epsilon_m Re[CM(\omega)]^2 r^2 E^2, \quad (3)$$

where the coefficient  $C$  depends on the distance between the particles and the length of the particle chain ( $3 < C < 10^3$ ).

AC-dielectrophoretic phenomena are an important field of research in biological and medical sciences with different model cells, mainly of mammalian origin (e.g., cancer cells, different cell-lines, and blood erythrocytes) as reviewed recently.<sup>6,7</sup> A few examples of chaining with unicellular organisms include: viable yeast collected using castellated microelectrodes<sup>10</sup> or two coplanar gold electrodes;<sup>8</sup> freshwater alga *Selenastrum capricornutum* collected with two needle electrodes<sup>12</sup> and *Eremosphaera viridis* collected on single metal microelectrode;<sup>13</sup> collecting of several bacteria species such as *Escherichia coli*, *Serratia marcescens*, *Pseudomonas aeruginosa*, *Bacillus subtilis*, *Staphylococcus aureus*, and *Salmonella*.<sup>14–16</sup> In addition to being a function of the dielectrophoretic “phenotype” of the particles and cells, the efficiency of the trapping, focusing, and separation depends on:<sup>6,7</sup> (i) the intensity of the applied electric field. For example, cells of *E. coli* have no reaction between 0 and 10 V and 0 to 20 MHz, whereas from 100 kHz and 20 MHz at 10 V, these cells are trapped at the edges of the interdigitated electrodes;<sup>17</sup> (ii) the frequency of the AC field. Several studies performed with unicellular organisms have shown the importance of the frequency in DEP separation between bacterium *Lactobacillus* and yeast *Saccharomyces cerevisiae* at 100 kHz,<sup>18</sup> between viable and nonviable *E. coli* at 1 MHz,<sup>14</sup> between dormant and active forms of *Mycobacterium smegmatis* at 120 kHz,<sup>19</sup> or between *Cryptosporidium muris* and *Giardia lamblia* at 10 MHz;<sup>20</sup> (iii) the geometry of the used electrodes. For example, long chains are produced in a field induced by two coplanar gold electrodes, whereas two dimensional arrays of particles form between four orthogonally arranged electrodes;<sup>8,21</sup> (iv) the (bio)particle size, shape and charge. For example, this has allowed the separation of yeast *S. cerevisiae* from bacterium *Micrococcus lysodeikticus* using interdigitated electrodes;<sup>22</sup> (v) the composition and concentration of the electrolyte in the medium. Different concentrations of amphoteres like  $\epsilon$ -aminocaproic acid or 4-(2-hydroxyethyl)-1-piperazineethanesulfonic acid (HEPES) have facilitated the negative DEP of yeast cells.<sup>23</sup> In most of the studies, experiments were performed in deionised water, Good’s buffers or blood plasma.<sup>7</sup> Overall, the specific combination of the above parameters controls the rate of cell capture and the morphology of the collected material.

Several DEP-based devices have been developed and applied in water quality assessment using different bioparticles,<sup>14,19,24,25</sup> however, very few studies have focused on DEP manipulation of live cells for realistic environmental biosensing and biodetection.<sup>3</sup> The DEP response of aquatic microorganisms in freshwaters is thus largely unexplored, and the potential of DEP as a tool for immobilization and analysis of live cells and contaminant particulates in environmental samples has not been fully assessed.

This study focuses on cell capture and immobilization in one-dimensional arrays by DEP. The major objective is to understand to what extent and under what conditions the composition of freshwaters could affect the dielectrophoretic response and thus influence the algal trapping and chaining in the microfluidic on-chip devices. Green microalga *Chlamydomonas reinhardtii* was chosen in this study, as a model unicellular organism representative for the freshwater phytoplankton used in the ecotoxicity tests. The influence of the electric field voltage and

frequency, and exposure time on the dielectrophoretic behavior of *C. reinhardtii* as well as the effect of the surface water composition on the cell trapping and chaining were explored. Both freshwaters and model systems with different chemical compositions were tested.

## II. MATERIALS AND METHODS

### A. Test media and algal cell cultures

Dielectrophoretic behavior of microalgal cells was characterized in freshwater samples from Rhône River, Laconnex Pond, and Geneva Lake. Their major cationic and anionic composition, pH, and dissolved organic matter (DOM) contents are listed in Table I. In addition, tests in model media were performed to understand better the effects of major cations and anions, as well as DOM typically found in surface waters, on the algal dielectrophoretic response. The composition of these model test media is presented in Table II.

Green alga *C. reinhardtii* (CPCC 11, Canadian Phycological Culture Centre, Waterloo, Canada) was grown at 20 °C under continuous light regime of 6000 lux and rotary shaking at 115 rpm (Multitron Shaking Incubator, INFORS HT, Basel, Switzerland) in a 4× diluted Tris-Acetate-Phosphate medium (4× TAP) (Sigma-Aldrich, Buchs, Switzerland) to the late exponential growth phase. The cells were isolated from the growth medium by gentle centrifugation at 3000 rpm for 10 min (Omnifuge 2.0 RS, Heraeus Sepatech GmbH, Osterode/Harz, Germany). The supernatant was discarded and the cells were re-suspended in the test medium to a concentration of  $10^6$  cells  $\text{ml}^{-1}$ .

### B. DEP experimental setup

DEP trapping and chaining experiments were performed with a coplanar gold electrodes separated by a 2 mm-gap, which were incorporated in a 250  $\mu\text{m}$  thick transparent microfluidic

TABLE I. Major cation and anion concentrations in the tested surface waters. The values are averaged over 3 measurements  $\pm$  standard deviations.

	Rhône River	Laconnex Pond	Geneva Lake
$\text{Ca}^{2+}$ ( $\times 10^{-3}\text{M}$ )	$1.1 \pm 0.2$	$2.7 \pm 0.1$	$1.1 \pm 0.05$
$\text{Mg}^{2+}$ ( $\times 10^{-3}\text{M}$ )	$0.20 \pm 0.01$	$0.33 \pm 0.02$	$0.25 \pm 0.02$
$\text{Na}^+$ ( $\times 10^{-3}\text{M}$ )	$0.23 \pm 0.03$	$0.19 \pm 0.02$	$0.27 \pm 0.01$
$\text{K}^+$ ( $\times 10^{-6}\text{M}$ )	$36.0 \pm 6.0$	$76.0 \pm 12.0$	$39.0 \pm 9.0$
DOM ( $\text{mg l}^{-1}$ )	$2.0 \pm 0.3$	$9.2 \pm 0.8$	$1.5 \pm 0.1$
$\text{Cl}^-$ ( $\times 10^{-3}\text{M}$ )	$0.24 \pm 0.1$	$0.19 \pm 0.1$	$0.25 \pm 0.2$
$\text{NO}_3^-$ ( $\times 10^{-3}\text{M}$ )	14	9.3	35
$\text{SO}_4^{2-}$ ( $\times 10^{-3}\text{M}$ )	$0.41 \pm 0.05$	$0.13 \pm 0.03$	$0.51 \pm 0.02$
pH	7.9	7.8	8.2

TABLE II. Composition of the tested model systems and concentration range. pH = 7.0.

	Concentration	
Citrate ( $\times 10^{-6}\text{M}$ )	1	1000
$\text{KH}_2\text{PO}_4$ ( $\times 10^{-6}\text{M}$ )	1	100
$\text{Ca}(\text{NO}_3)_2$ ( $\times 10^{-5}\text{M}$ )	1.7	17
MOPS ( $\times 10^{-4}\text{M}$ )	1	10
$\text{NaNO}_3$ ( $\times 10^{-4}\text{M}$ )	1	10
SRHA <sup>a</sup> ( $\text{mg l}^{-1}$ )	5	20

<sup>a</sup>SRHA—Suwannee River humic acid in  $10^{-3}\text{M}$  MOPS.

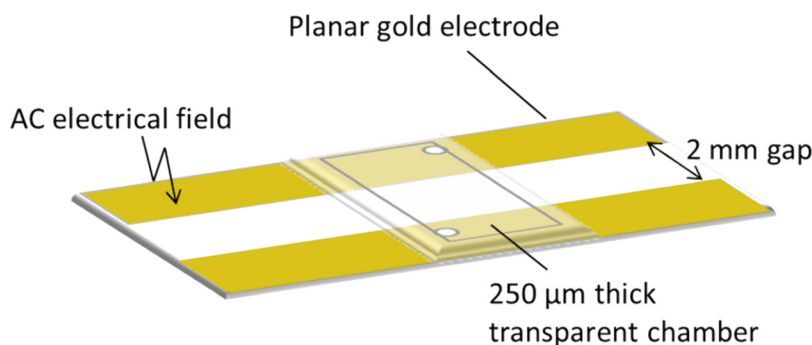


FIG. 1. Schematics of the microfluidic chamber with two coplanar gold electrodes used for dielectrophoretic trapping and chaining of algal cells.

chamber (HybriWell Incubation Chamber, BioCat GmbH, Heidelberg, Germany) (Fig. 1). The gold electrodes were vapor-deposited onto  $25 \times 75$  mm microscope glass slides (Fisher Scientific, Pittsburgh, USA) as described elsewhere.<sup>21,26</sup> Coplanar electrodes were chosen because of their capacity to trap and chain cells while allowing for easy microscope display.<sup>8</sup> This design with large gap was also preferred due to its simplicity, robustness, and uniform field. These electrodes were connected to a generator (33220 A Function/Arbitrary Waveform Generator, 20 MHz, Agilent Technologies SA, Morges, Switzerland) through a voltage amplifier (2340 Single Channel Amplifier, Tegam, Geneva, USA). The electric signal was continuously followed by an oscilloscope (Analogical oscilloscope 630-2 ( $2 \times 30$  MHz), Voltcraft, Zurich, Switzerland). The frequencies used were limited to a maximum of 1 kHz to avoid distortion of the AC signal by the amplifier loaded with the highly capacitive cell.

To follow algal chaining in different medium, *C. reinhardtii* cells suspended in different test media were injected into the chamber and an AC-field was applied. The frequency and the voltage of the AC-field were varied by using a  $2^2$  experimental design. Based on preliminary experiments, the following combinations of frequency and voltage were tested: low frequency and voltage of 200 Hz and  $10 \text{ V mm}^{-1}$ , high frequency and voltage of 1 kHz and  $20 \text{ V mm}^{-1}$ , low frequency and high voltage of 200 Hz and  $20 \text{ V mm}^{-1}$ , and high frequency and low voltage of 1 kHz and  $10 \text{ V mm}^{-1}$ . After each experiment, the microfluidic chamber was thoroughly flushed 5 times with  $50 \mu\text{l}$  of deionised water to eliminate all residues of the previous media.

### C. Microscopy and image analysis

The DEP behavior of the cells in the microfluidic chamber was observed with optical microscope (BX61, OLYMPUS, Volketswil, Switzerland) using a digital camera (XC30, OLYMPUS Volketswil, Switzerland) and the CELLSSENS software (Cellsens dimension OLYMPUS Volketswil, Switzerland) provided. For each combination of voltage, frequency, and test medium, images were collected at 30 s, 45 s, 60 s, and then every 30 s until 600 s following the AC-field application. The efficiency of chain formation was characterized by the percentage of cells in chains and the length of chains determined by using the image processing program IMAGEJ (National Institute of Mental Health, Bethesda, USA). The percentage of cells in chains was calculated for each image according to

$$\% \text{ of cells in chains} = \frac{\sum \text{number of chains} * \text{number of cells per chain}}{\text{total number of cells in the system}}. \quad (4)$$

For each condition, three replicate measurements were performed, the mean of the percentage of cells in chain and the standard deviation were calculated and compared.

#### D. AC-field effect on *C. reinhardtii*

To determine if AC-fields affect *C. reinhardtii* viability characteristics, algal autofluorescence, cell membrane integrity, and reactive oxygen species-induced damages in the algae were determined prior and after the application of the AC-field for 600 s. The effect of AC-field on membrane integrity was measured using propidium iodide (PI, Life Technologies Europe B.V, Zug, Switzerland). 10  $\mu$ l of 700  $\mu$ M solution of PI was added to 1 ml suspension of *C. reinhardtii* in 3-(N-morpholino)propanesulfonic acid (MOPS) after AC-field applied for 600 s. The mixture was kept in at room temperature in dark for 15 min, then washed, and analyzed by fluorescence microscopy and flow cytometry (BD Accuri™ C6, BD Biosciences, San Jose, USA). To probe the possible lipid peroxidation damages induced by electric field, 2.5  $\mu$ l of 1 mM of lipophilic fluorescent dye 4,4-difluoro-5-(4-phenyl-1,3-butadienyl)-4-bora-3a,4a-diaza-s-indacene-3-undecanoic acid (C11-BODIPY<sup>581/591</sup>) were added to 1 ml of cell suspensions. After incubation for 45 min, the algal cells were analyzed by fluorescence microscopy and flow cytometry.

#### E. Measurement of conductivity of algal suspensions and cell zeta potential

To interpret the impact of the medium on the DEP properties of the cells, the electrophoretic mobility,  $\zeta$ -potential, and conductivity of the algal suspensions were measured by electrophoretic light scattering (Zetasizer Nano ZS, Malvern, Worcestershire, United Kingdom). The mean and the standard deviation of each parameter were calculated based on the results obtained with three replicates (Table III).

### III. RESULTS AND DISCUSSION

#### A. Effect of the electrical field parameters on cell chaining

The algal cells suspended in freshwater and model medium began aligning and forming one dimensional chain arrays in the direction of the applied AC-field within 45 s (Fig. 2). However, the percentage of cells captured in the chains and the chain length were medium-dependent. For example, for a field intensity of 10 V mm<sup>-1</sup> and frequency of 200 Hz, one dimensional cell arrays were assembled after 45 s in 10<sup>-3</sup>M MOPS, 1.7  $\times$  10<sup>-5</sup>M Ca(NO<sub>3</sub>)<sub>2</sub>, 10<sup>-6</sup>M citrate, and 10<sup>-6</sup>M KH<sub>2</sub>PO<sub>4</sub>, but not in 10<sup>-4</sup>M NaNO<sub>3</sub>, 10<sup>-3</sup>M MOPS + Suwannee River humic acid (SRHA), and water from Geneva Lake (Fig. 2(a)). Small chains of 3 to 4 cells each were formed for both frequencies and field intensity of 10 V mm<sup>-1</sup> (Figs. 2(a) and 2(b)). The increase of the frequency of AC-field from 200 Hz to 1 kHz resulted in an increase of the percentage of cells collected in chains in the studied media with exception of 10<sup>-6</sup>M of

TABLE III. Zeta potential ( $\zeta$ ), electrophoretic mobility ( $\mu$ ), and conductivity ( $\sigma$ ) of *C. reinhardtii* suspensions in surface waters and simple model media. The values are mean of 3 replicates and standard deviations.

	$\zeta$ (mV)	$\mu$ ( $\mu$ m cm V <sup>-1</sup> s <sup>-1</sup> )	$\sigma$ ( $\mu$ S cm <sup>-1</sup> )
Geneva Lake	-15.8 $\pm$ 1.0	-1.2 $\pm$ 0.1	320.0 $\pm$ 3.5
Laconnex Pond	-14.2 $\pm$ 1.2	-1.1 $\pm$ 0.1	560.0 $\pm$ 7.1
Rhône River	-13.8 $\pm$ 0.3	-1.1 $\pm$ 0.0	385.0 $\pm$ 3.0
10 <sup>-3</sup> M MOPS	-31.0 $\pm$ 1.1	-2.4 $\pm$ 0.1	36.8 $\pm$ 0.4
10 <sup>-3</sup> M Citrate	-30.2 $\pm$ 0.1	-2.4 $\pm$ 0.1	258.7 $\pm$ 1.5
10 <sup>-6</sup> M Citrate	-30.8 $\pm$ 2.1	-2.4 $\pm$ 0.2	41.4 $\pm$ 2.2
10 <sup>-4</sup> M KH <sub>2</sub> PO <sub>4</sub>	-30.9 $\pm$ 2.7	-2.4 $\pm$ 0.2	72.7 $\pm$ 0.4
10 <sup>-6</sup> M KH <sub>2</sub> PO <sub>4</sub>	-28.7 $\pm$ 1.1	-2.3 $\pm$ 0.1	69.2 $\pm$ 0.4
1.7 $\times$ 10 <sup>-4</sup> M Ca(NO <sub>3</sub> ) <sub>2</sub>	-18.4 $\pm$ 1.0	-1.4 $\pm$ 0.1	60.4 $\pm$ 0.4
1.7 $\times$ 10 <sup>-5</sup> M Ca(NO <sub>3</sub> ) <sub>2</sub>	-25.3 $\pm$ 0.7	-2.0 $\pm$ 0.1	24.8 $\pm$ 4.6
10 <sup>-4</sup> M NaNO <sub>3</sub>	-29.2 $\pm$ 0.9	-2.3 $\pm$ 0.1	181.7 $\pm$ 1.5
10 <sup>-3</sup> M MOPS + 5 ppm SRHA	-29.6 $\pm$ 1.0	-2.3 $\pm$ 0.1	81.0 $\pm$ 2.1
10 <sup>-3</sup> M MOPS + 20 ppm SRHA	-27.0 $\pm$ 0.7	-2.1 $\pm$ 0.1	168.0 $\pm$ 1.0

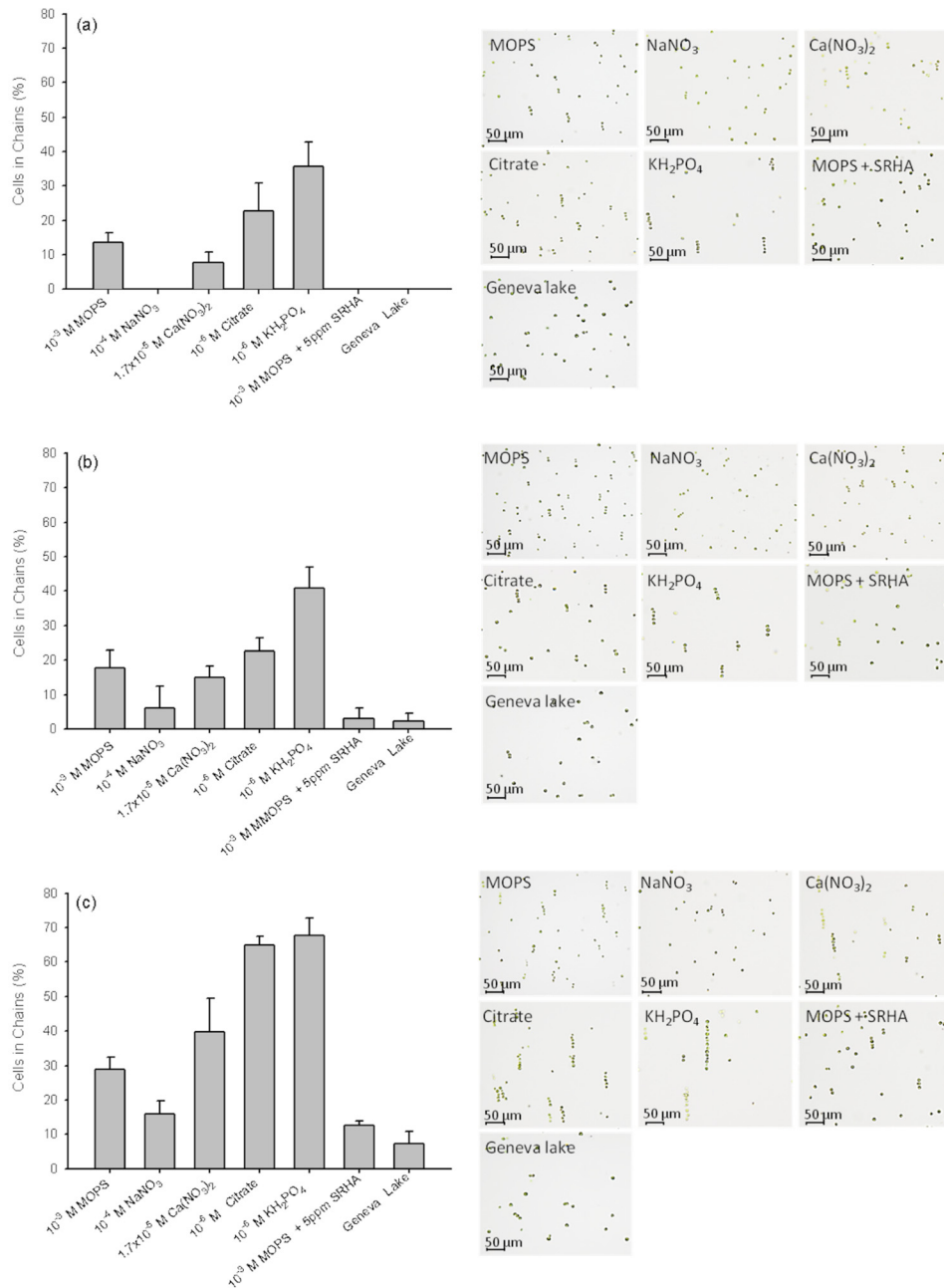


FIG. 2. Effect of the AC-field intensity and frequency on chaining of *C. reinhardtii* suspended in different test media after the AC-field was applied for 45 s. Left: Percentage of cells captured in chains under voltage/frequency combinations of (a) 10 V mm<sup>-1</sup> and 200 Hz; (b) 10 V mm<sup>-1</sup> and 1 kHz; and (c) 20 V mm<sup>-1</sup> and 1 kHz. Right: Microscope images illustrating the chain structure and length for each combination of field intensity and frequency.

citrate or KH<sub>2</sub>PO<sub>4</sub>. It is also induced chaining in Geneva Lake water and media containing 10<sup>-4</sup>M NaNO<sub>3</sub> and 10<sup>-3</sup>M MOPS + SRHA within 45 s (Fig. 2(b)). Nevertheless, given the relatively low frequencies used in the study dictated by the wide gap electrodes set-up, we expect that the increase of the chaining efficiency with the frequency arises from more complex and yet poorly understood electrokinetic effects involving the ionic species at or near the cell surfaces.<sup>27</sup> A reliable evaluation of the effect of frequency higher than 10 kHz on cell chaining was not possible with this electrode configuration because of the distortion of the high voltage AC signal by the amplifier loaded with the highly capacitive cell. The use of large gap DEP cell,



however, has a number of other advantages, which are important in cell chaining: (i) these electrodes are simple to implement, inexpensive and allow using larger microchambers, (ii) they create a uniform field over large distances, where the even horizontal component is larger than the non-uniform vertical projection of the field, (iii) they allow facile observation of the process of algal chaining in common transmitted microscopy mode without electrode background, and (iv) they are much less influenced by AC electrothermal and electrohydrodynamic effects at the electrode edges, which could create significant artifacts and damage the algal cells.

The increase of the AC-field intensity from  $10 \text{ V mm}^{-1}$  to  $20 \text{ V mm}^{-1}$ , which is the main DEP chaining driving force (Eq. (2)), resulted in a significant improvement of the cell chaining efficiency (Fig. 2(c)). The percentage of cells in chains increased 1.5 to 4-fold. In most of the cases, the formed chains consisted of 6 to 7 cells. Moreover, the chain assembling process was reversible and the chains came apart after the electric field was turned off. The above results are consistent with the existing literature for yeast cells, bacteria, and protozoa<sup>7,8,14,20,28</sup> demonstrating an increase of cell chaining with AC-field intensity. For example, the increase of the voltage from  $5 \text{ V mm}^{-1}$  to  $20 \text{ V mm}^{-1}$  produced an increase of the average cell chain length of baker's yeast cell at all studied frequencies.<sup>8</sup> Similarly, the increase of the AC-field intensity from  $67 \text{ V cm}^{-1}$  to  $84 \text{ V cm}^{-1}$  increased the capture efficiency from 90% to 99% for bacteria *E. coli*, *Salmonella*, and *Pseudomonas* sp.<sup>14</sup>

No chain formation was observed in all studied media at the combination of low frequency of 200 Hz and high field intensity of  $20 \text{ V mm}^{-1}$  because of fluid AC-electroosmosis (ACEO) and the fluid flow generated near the electrodes that disrupted the chain formation (data not shown). In ACEO, the applied potential between the electrodes induces a fluid motion which drags the particles,<sup>28</sup> as reported earlier with latex particles at low frequencies.<sup>9,29</sup> Indeed, at frequencies below 100 Hz, cells begin to vibrate as they follow the direction of the field and macroscopic fluid currents circulate inside the chamber and disrupt the homogeneous layer of bioparticles on the bottom of the chamber.<sup>9</sup> However, in the case of yeast, the formation of longer chains was also observed at high voltages  $20 \text{ V mm}^{-1}$  and at low frequencies below 200 Hz,<sup>8</sup> which demonstrated the cell-specific dielectrophoretic phenotype and the importance of determining optimal combination of field intensity and frequency.

The effect of the duration of the applied AC-field on the kinetics and efficiency of cell chaining was also characterized. As shown in the example of MOPS in Fig. 3, prolongation of the AC-field application from 45 s to 600 s resulted in about 3-fold increase in the percentage of cells in chain with the AC field for both field intensities of  $10 \text{ V mm}^{-1}$  and  $20 \text{ V mm}^{-1}$  and frequency of 1 kHz. This observation is in broad agreement with literature results showing that the number of DEP-accumulated DNA nanoparticles<sup>30</sup> or latex particles<sup>28</sup> increases with time and field magnitude. Interestingly, for a given time, the number of formed chains increased at higher voltage, while the chain length was similar at both  $10 \text{ V mm}^{-1}$  and  $20 \text{ V mm}^{-1}$ . Indeed, the initial rate of chaining estimated as the slope of the dependence of the percentage of cells in chains and time until 90 s (Fig. 3(a)) increased 4×, when the applied voltage doubled in agreement with the Eq. (2). At longer times (i.e., 330 s), the doubling of the voltage only leads to a 2-fold increase in the percentage of cells in chains. The decrease of the rate of cell chain growth likely reflects the transition between the original rapid assembly driven by forces alone and the later stages controlled by the rate of diffusion of the cells.

## B. Cell capture and assembly in freshwaters

Dielectrophoretic response of algae was explored in freshwater sampled from Geneva Lake, Laconnex Pond, and Rhône River. The DEP response of algae in samples from Geneva Lake and Rhône River was found to be similar (Figs. 4(a) and 4(b)). About 43% of the cells from these suspensions were assembled in 1-D arrays of 4 to 5 cells each 600 s after applying the AC-field of  $20 \text{ V mm}^{-1}$  and 1 kHz. The assembly process was rapid and a small number of short chains were already observed after 45 s. At lower AC-field intensity of  $10 \text{ V mm}^{-1}$ , no cell chaining was observed after 45 s and less than 10% of the cells formed chains after 600 s, as expected by the lower dielectrophoretic forces. The suspensions of *C. reinhardtii* in

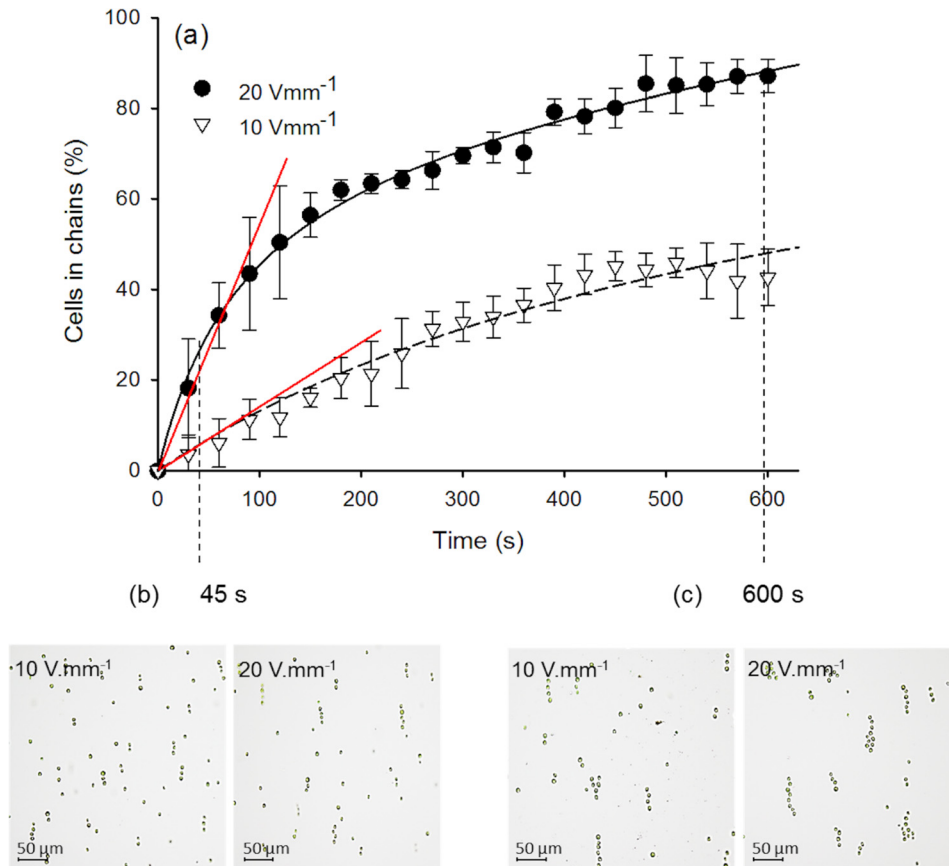


FIG. 3. Effect of the AC-field duration on the collection of the algal cells in chains (a) and on the chain structure at different voltages in  $10^{-3}$  M MOPS ((b) and (c)). (a) Kinetics of cells collection in chains for 10 and 20 V mm<sup>-1</sup>. The signal frequency was 1 kHz. Optical micrographs of algal chains assembled after 45 s (b) and 600 s (c) for AC-field intensity of 10 and 20 V mm<sup>-1</sup>. Initial slope used as a measure of the initial rate of chaining is given in red.

Laconnex Pond (Fig. 4(c)) exhibited no cell chain assembly at 10 V mm<sup>-1</sup> and 1 kHz. Algal chains were only formed at higher field intensity of 20 V mm<sup>-1</sup> and 1 kHz. Interestingly, algal cells begin aligning after 120 s in Laconnex Pond samples and the percentage of cells in chains increases up to  $47.8 \pm 4.7\%$  after 600 s, a value comparable to those determined in sample from Geneva Lake and Rhône River. Nonetheless, the efficiency of cell formation was lower as compared to the 87% of the cells in chain formed in biological buffer MOPS after 600 s at 20 V mm<sup>-1</sup> and 1 kHz. Estimation of initial rates of chain formation for Geneva Lake and Rhône River demonstrated that doubling of the applied field resulted to a 1.5-2-fold rather than theoretically expected 4-fold increase of the chaining efficiency. The complex multitude of ionic and surface active compounds present in the freshwaters could possibly slow the initial cell chaining, while ultimately leading to good collection as explained further.

### C. Cell assembly in model media

To gain further insight on the effect of common compounds that can be found in freshwaters on the algal assembly by DEP, simple model media containing different concentrations of major cations—Ca<sup>2+</sup>, Na<sup>+</sup> or anions—nitrate, phosphate, and citrate were tested. SRHA was used as a representative DOM with concentrations of 5 and 20 ppm. The efficiency of cell capture and assembly at 20 V mm<sup>-1</sup> and 1 kHz was compared at 45 s and 600 s after the application of the electrical field. For all the model media, the percentage of cells in chain and the chain length increased with the duration of AC-field (Fig. 5) in a medium-dependent way. After 600 s, around 80% of cells were aligned in 1D-arrays in  $1.7 \times 10^{-5}$  M Ca(NO<sub>3</sub>)<sub>2</sub>,  $10^{-6}$  M citrate,



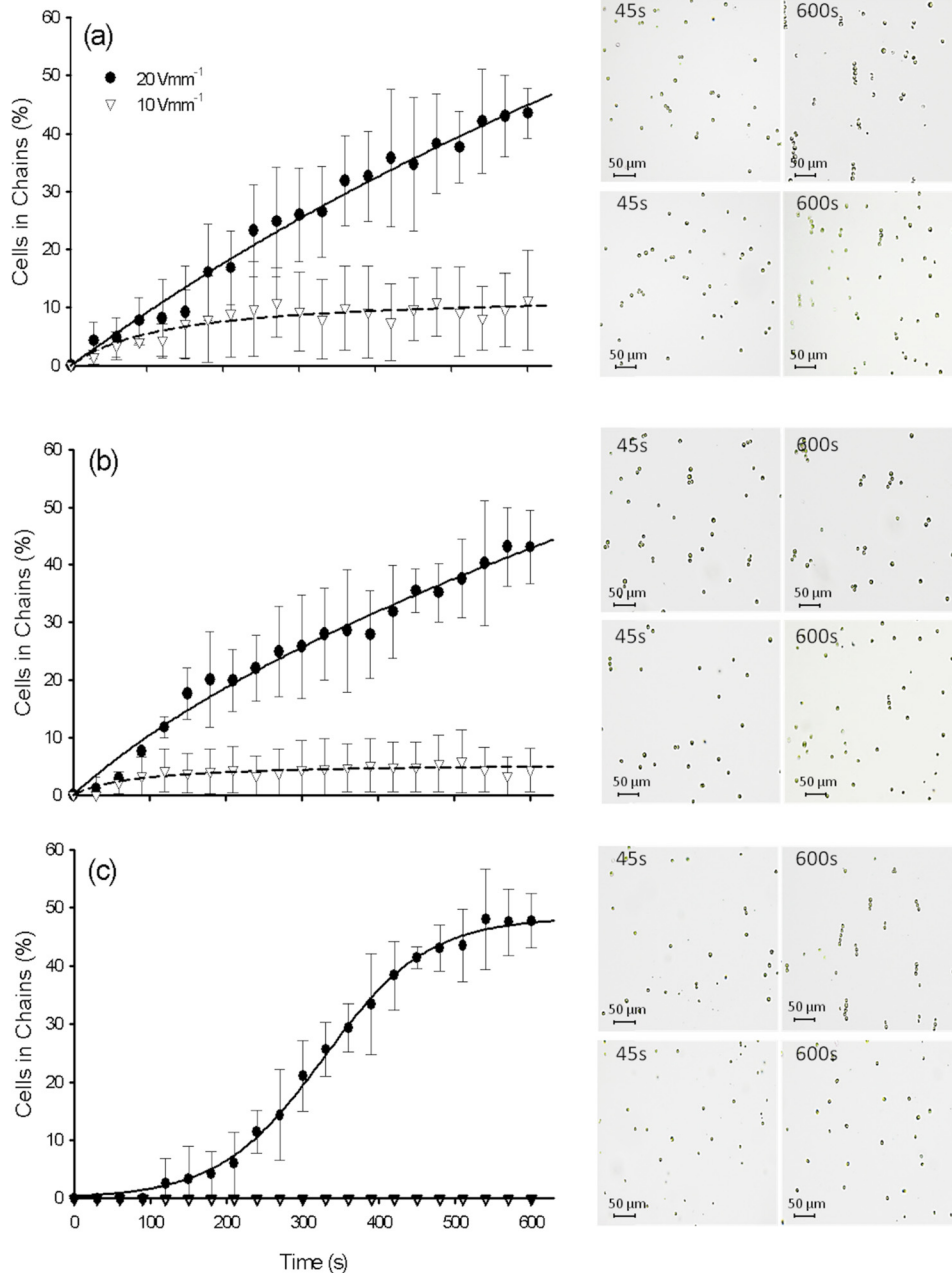


FIG. 4. Collection of cells of *C. reinhardtii* in freshwaters and structure of the chains as a function of time. The graphs represent the percentage of chained cells at 10 and 20 V mm<sup>-1</sup> in water from Geneva Lake (a), Rhône River (b), and Lacconnex Pond (c). The optical micrographs show the structure of the chains at 45 s and 600 s for both voltages. The frequency was 1 kHz in all experiments.

and 10<sup>-4</sup>M KH<sub>2</sub>PO<sub>4</sub>, whereas this percentage was about twice lower in 10<sup>-4</sup>M citrate and 5 ppm SRHA in MOPS. DEP efficiency was low, corresponding to less than 10% of cells in chains in medium containing 10<sup>-4</sup>M NaNO<sub>3</sub> or 20 ppm SRHA. No cell assembly and electrode damage was observed in medium containing 1.7 × 10<sup>-4</sup>M Ca(NO<sub>3</sub>)<sub>2</sub>. The percentage of cells in chains followed the tendency: 10<sup>-4</sup>M KH<sub>2</sub>PO<sub>4</sub> > 1.7 × 10<sup>-5</sup>M Ca(NO<sub>3</sub>)<sub>2</sub> ~ 10<sup>-6</sup>M Citrate ~ 10<sup>-6</sup>M KH<sub>2</sub>PO<sub>4</sub> ~ 5 ppm SRHA > 10<sup>-3</sup>M Citrate ≫ 20 ppm SRHA > 10<sup>-4</sup>M NaNO<sub>3</sub>. The length of cell assemblage decreases in the order: 10<sup>-4</sup>M KH<sub>2</sub>PO<sub>4</sub> ~ 10<sup>-6</sup>M KH<sub>2</sub>PO<sub>4</sub> ≫ 1.7 × 10<sup>-5</sup>M Ca(NO<sub>3</sub>)<sub>2</sub> > 10<sup>-6</sup>M citrate ≫ 10<sup>-3</sup>M citrate > 5 ppm SRHA ≫ 20 ppm SRHA and 10<sup>-4</sup>M NaNO<sub>3</sub>.

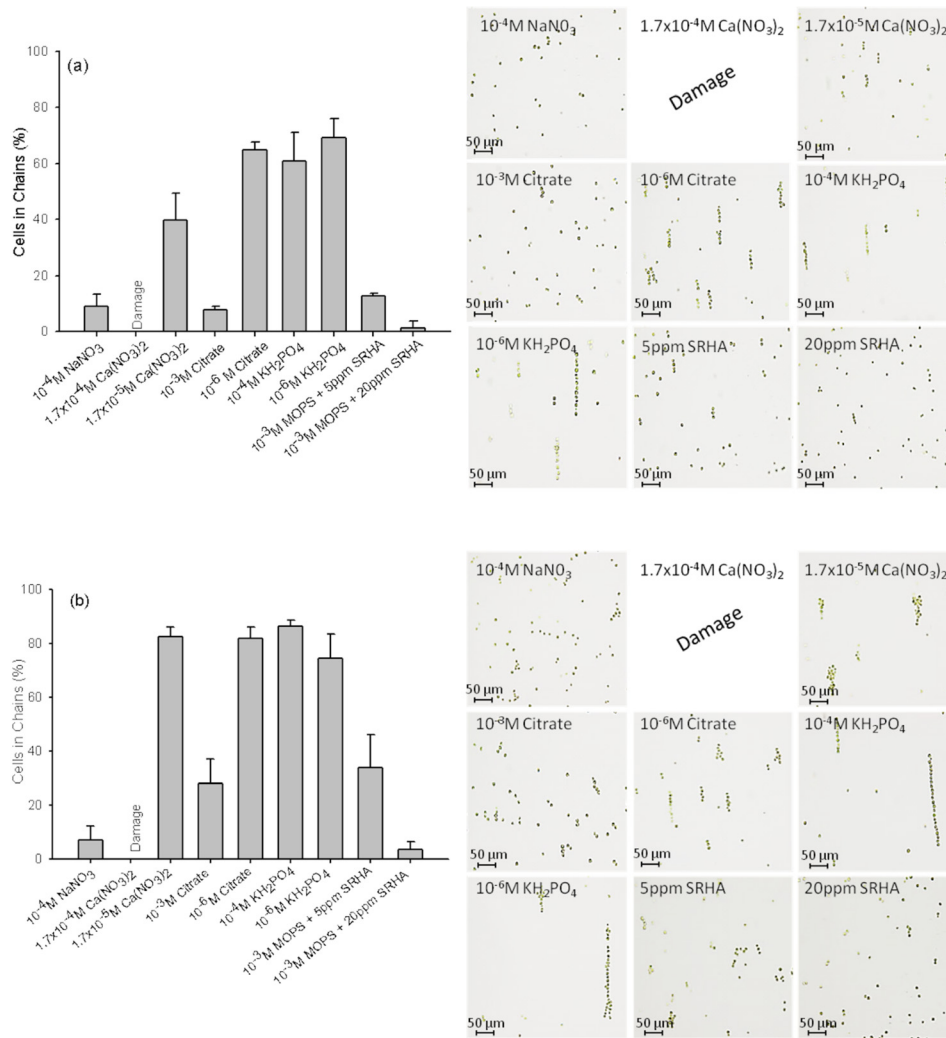


FIG. 5. Effect of the medium on the collection of cells of *C. reinhardtii* and structure of the chains at 45 s (a) and 600 s (b). The graphs represent the percentage of cells in chain at  $20 \text{ V mm}^{-1}$  and 1 kHz. The optical micrographs show the structure of the chains at 45 s and 600 s for each model system.

To better understand the effect of the media on the dielectrophoretic “phenotype” of *C. reinhardtii* cells, the correlations between the chaining efficiency and conductivity of the algal suspensions were also evaluated. The efficiency of DEP assembling correlated negatively with the conductivity in different model media (Fig. 6(a)). The highest percentages of cell chaining were obtained in model media with conductivities below  $80 \mu\text{S cm}^{-1}$ . The decrease of the chaining efficiency with the increase of medium conductivity is in line with the existing numerous literature about the DEP of yeast cells, as well as blood, lung, or breast cancer and HT-29 cells.<sup>6,7</sup> A decrease in the efficiency of DNA collection with an increase of buffer’s conductivity has also been observed.<sup>30</sup> The chaining rate (i.e., number of cells added per unit time) and the chain length in the model media could be expected to be proportional to the chaining force  $F_{chain}$ . For a given frequency and field strength  $F_{chain}$  should depend of the conductivity of the medium through the Clausius-Mossotti factor

$$-F_{chain} \frac{1}{C\pi\epsilon_m r^2 E^2} = \text{Re}|CM(\omega)|^2. \quad (5)$$

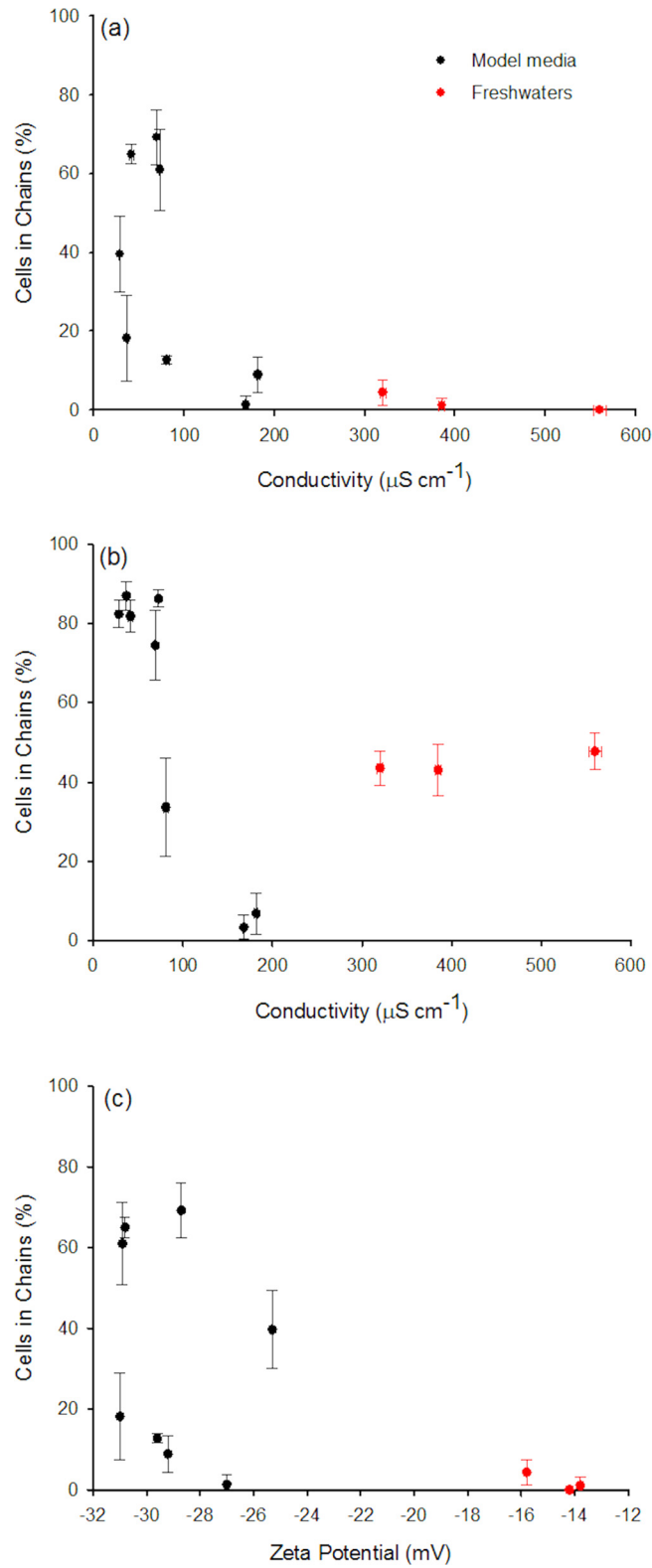


FIG. 6. Percentage of cells in chains at 45 s (a) and 600 s (b) in different media versus the conductivity of cell suspensions. The data at 600 s point out to abnormally high rate of chain formation. (c) Percentage of cells in chains vs. the cell zeta potential. AC-field intensity of  $20 \text{ V mm}^{-1}$  and frequency of 1 kHz.

The increase of the conductivity of the medium would result in a decrease in the complex permittivity of the medium  $\epsilon_m^*$  and in the real part of  $Re[CM(\omega)]^2$  leading to a decrease of the efficiency of chaining. This is indeed the case: the corresponding calculations of the cell polarizability and re-plotted data from Fig. 6 are given in the supplementary material.<sup>31</sup> Interestingly, the DEP “phenotype” of cells in the three freshwater samples shows significant differences at larger times than the one observed in the model media (Fig. 6(b)). The alga in freshwater exhibited abnormally high degree of chaining at longer times (Fig. 6(b)).

The chaining behavior may in theory be correlated to the  $\zeta$ -potential of the cells, since it controls the ionic density in the Stern layer<sup>32</sup> and thus affects bioparticle DEP polarization. At pH of 7.0–8.2 used in the present study, the  $\zeta$ -potential of algae has negative values, which is affected by the presence of different compounds in the test media. The algal  $\zeta$ -potential decreased in the order  $10^{-4}\text{M KH}_2\text{PO}_4 \sim 10^{-6}\text{M citrate} \sim 10^{-3}\text{M citrate} > 5\text{ ppm SRHA} \sim 10^{-4}\text{M NaNO}_3 > 10^{-6}\text{M KH}_2\text{PO}_4 > 20\text{ ppm SRHA} > 1.7 \times 10^{-5}\text{M Ca(NO}_3)_2 \gg 1.7 \times 10^{-5}\text{M Ca(NO}_3)_2 > \text{Geneva Lake} > \text{Laconnex Pond} \sim \text{Rhône River}$ . The  $\zeta$ -potential (and algal charge) can influence cellular DEP behavior through electrophoretic contribution, counter ion relaxation, and conduction in algal double layer surrounding.<sup>6,16</sup> The values of the  $\zeta$ -potential affect the counter-ionic layer conductivity and permittivity, and thus, the chaining force via  $Re[CM(\omega)]^2$  (see Eq. (S6) in the supplementary material<sup>31</sup>). Model calculations were performed to evaluate the effect of the  $\zeta$ -potential on the complex permittivity of the counter-ionic layer (Eq. (S1)).<sup>31</sup> No significant effect on  $F_{chain}$  and  $Re[CM(\omega)]^2$  was found when taking into account the counter-ionic layer contribution.<sup>31</sup> Thus, it is likely that the  $\zeta$ -potential has insignificant influence on algal chaining at frequency of 1 kHz and electric field force of  $20\text{ V mm}^{-1}$ . Such conclusions are in line with a previous report that showed a negligible effect of  $\zeta$ -potential on the relative motion of particles in an AC-field.<sup>33</sup> Our data show, however, that the complex chemical composition (e.g., presence of macronutrients such as  $\text{Ca}^{2+}$  and phosphate and amphiphilic humic substances) and slightly different pH in natural waters (pH 7.8–8.2) as compared to model media (pH = 7.0) have a noticeable effect on chaining. The effect of pH and media composition on the pronounced chaining at long times (Fig. 6(b)) is likely to originate not only in the changes in the charge of the cell surface (accounted in  $\zeta$ -potential and proved to be of little impact by modeling) but also the ion concentration and compositions in the double layer as well as the complex cellular structure and metabolic changes that the three shell model does not take into account.<sup>6</sup>

The results obtained in model media suggest that the presence of phosphate and calcium, essential cell nutrients, at concentrations relevant to freshwaters could favor the cell assembly process and result in longer chain formation. By contrast, nitrate concentrations larger than  $10^{-4}\text{M}$  seem to interfere with DEP and inhibit algal chaining. Indeed, high nitrate concentrations were found to influence the medium ionic strength (as well as the conductivity) and thus cell DEP behavior. Furthermore, comparison of the percentage of the cells in chain and their length in MOPS in the absence (Fig. 3) and presence of SRHA (Fig. 5(b)), demonstrated that SRHA interferes with cells assembly and decreases the DEP efficiency, which was more pronounced with the increase of the SRHA concentration. This is in agreement with the existing literature showing that the adsorption of humic acids on algae can alter the algal surface charge, membrane permeability and  $^{14}\text{C}$  sorbitol uptake.<sup>34,35</sup>

Taken together the results obtained in surface waters and model media suggest that with the specific electrode configuration used in this study, high concentrations of the nitrate, phosphate, and dissolved organic matter present in surface waters could strongly affect the efficiency of DEP cell capture in chains. Indeed, nitrate ion concentrations of the order of  $10^{-2}\text{M}$  present in samples from Geneva Lake, Laconnex Pond, and Rhône River could be expected to decrease the efficiency of the cell chaining. Furthermore, relatively high concentrations of DOM could result in a lag of the cell alignment, as illustrated for Laconnex Pond water containing  $5\times$  more DOM than samples from Geneva Lake and Rhône River. However, even if the conductivity of the cells suspensions was high ( $>300\mu\text{S cm}^{-1}$ ) in the surface waters, chaining and trapping of the cells still occurred. It appears that some common ionic compounds present in the three waters such as phosphate or calcium ions (Table I) may not suppress much or

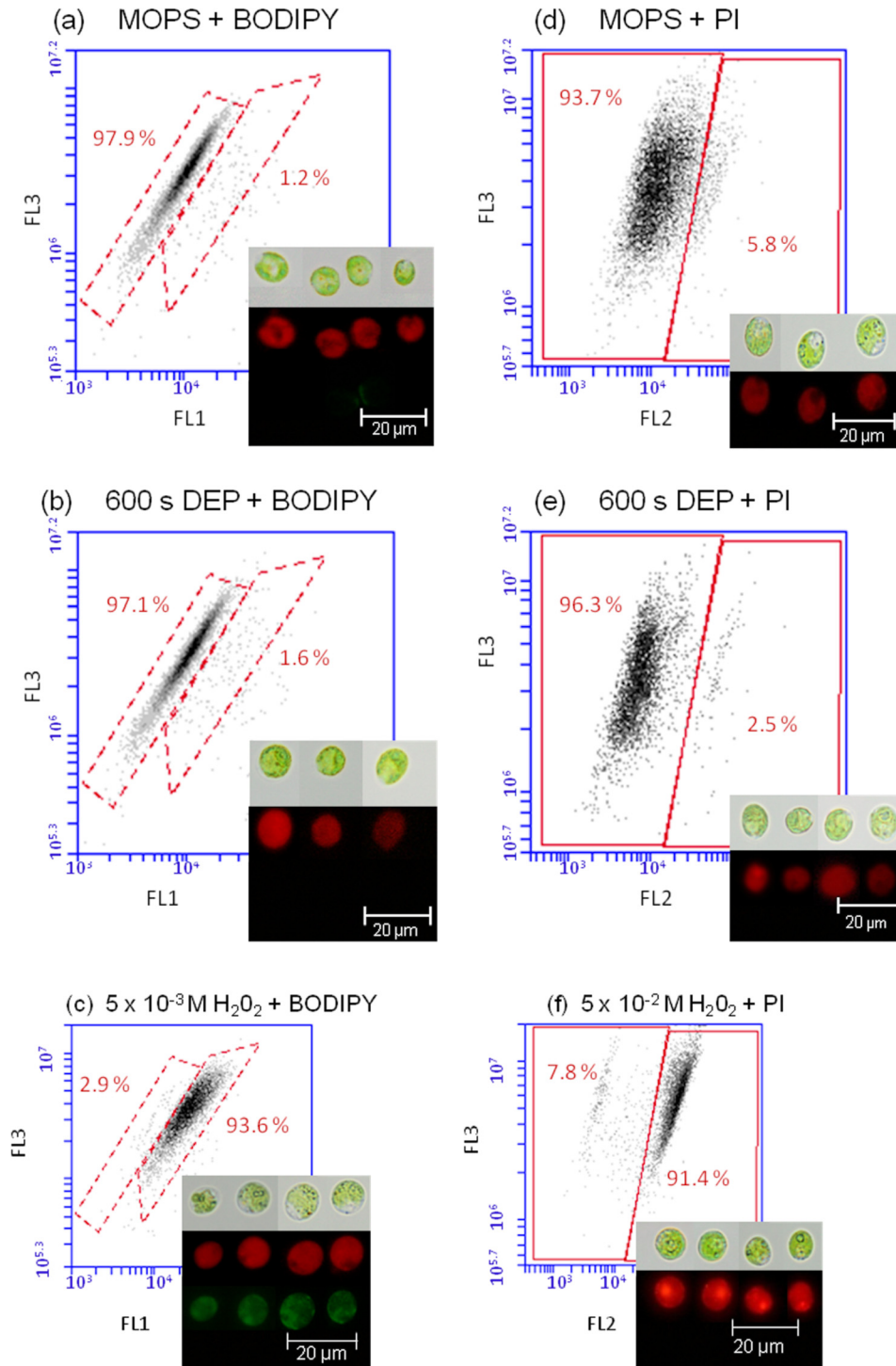


FIG. 7. Effect of DEP on the *C. reinhardtii* lipid peroxidation status ((a)–(c)) and membrane integrity ((d)–(f)) obtained by flow cytometry prior DEP ((a) and (d)) after 600 s of DEP ((b) and (e)) and after treatment with pro-oxidant  $5 \times 10^{-3}$  M H<sub>2</sub>O<sub>2</sub> ((c) and (f)). Two dimensional dot plots represent algal autofluorescence (FL3) versus fluorescence signal of BODIPY (FL1) or PI (FL2). Micrographs ((a)–(c)) obtained with fluorescence microscopy represent (up to down): algae observed with the bright field, algae observed with the fluorescent filter allowing the detection of chlorophyll *a* (red), and algae observed with the fluorescent filter allowing the detection of BODIPY (green). Micrographs ((d)–(f)) show algae observed with the bright field and algae observed with the fluorescent filter allowing the detection of chlorophyll *a* and PI (red). Medium  $10^{-3}$  M MOPS, pH = 7.0.

may even enhance cell chaining. One hypothesis for the physical origin of this effect may be the increased surface conductance of the counterionic layers containing multivalent ions, however, the intricate details of the cell counterion polarization and DEP response are a rather complex topic that will be subject of future investigations.

#### D. Cell physiology under DEP

The critical issue in the development of different live cell based sensors is that the DEP cell collection and chaining should not affect the cell physiology. The literature suggests that the electric field does not affect the viability of yeast,<sup>8</sup> endothelial cell,<sup>36</sup> or different mammalian cells,<sup>6</sup> however, no such information is available for green algae. In principle, DEP could be supplemented by cell damage due to joule heating of the medium, induction of transmembrane potential, or mechanical deformation.<sup>7</sup> In addition, the electric field could penetrate the outer cell membrane and induce a movement of the internal organelles, as chloroplasts move towards the electrode tip for alga *E. viridis*.<sup>13</sup> To verify if the DEP affect the *C. reinhardtii*, the influence of the AC-field on the algal autofluorescence, cell membrane damage, and ROS induced damages such as lipid peroxidation, which could affect cell permittivity, were determined. No measurable effect of the AC-field applied for 600 s on algal autofluorescence, membrane integrity, and lipid peroxidation was found (Fig. 7). The percentage of *C. reinhardtii* cell exhibiting leaky or damaged membranes was comparable prior (5.8%) and after (2.3%) application of the AC-field with a voltage of 10 or 20 V mm<sup>-1</sup> and frequency of 1 kHz for 600 s. Similarly no significant difference in the percentage of cells experiencing lipid peroxidation was found prior (1.2%) and after (1.6%) DEP assembly. This observation was further confirmed by the fluorescent microscopy (Fig. 7(b)), showing no green fluorescence corresponding to BODIPY after AC field DEP application. Furthermore, no effect of the applied AC-field on the algal autofluorescence was observed. These results demonstrated the AC-field has no significant effect on the cell physiology and in more general plan confirm the potential of this technique for trapping and immobilization of viable cells in biosensing devices.

#### IV. CONCLUSIONS

The results demonstrate the potential of the AC dielectrophoresis as a rapid and non-damaging tool for the capture and chain assembly of freshwater algal cells. Electric field operating conditions, such as AC-field frequency and intensity, as well as duration of the applied field, were shown to play important role in cell chaining. Highest percentage of chained cells and formation of longest chains were observed at 20 V mm<sup>-1</sup> and 1 kHz field applied for 600 s. Somewhat unexpectedly, we found that phosphate and calcium favor cell assembly and formation of longer chains. The efficiency of DEP-driven cell alignment in surface water samples representative for lake, pond, and river waters was strongly affected by chemical composition of the media and to some extent by the conductivity of the cells suspensions. High concentrations of nitrate, DOM, and the overall high conductivity in surface water could be expected to decrease cell chaining efficiency, but the changing in surface water over long periods was found to be higher than the model systems with corresponding conductance. Thus, it appears that subtle effects of medium composition and AC electrohydrodynamics could affect and potentially enhance the chaining in surface waters.

#### ACKNOWLEDGMENTS

The authors gratefully acknowledge the financial contribution of the Foundation Marc Birkigt of the University of Geneva and partial support from US-NSF Grant No. CBET-0828900 and US-NSF Triangle MRSEC on Programmable Soft Matter (DMR-1121107). We thank Elizabeth Melvin and Bhuvnesh Bharti for experimental assistance.

<sup>1</sup>C. Durrieu, C. Tran-Minh, J. M. Chovelon, L. Barthet, C. Chouteau, and C. Vedrine, *Eur. Phys. J.: Appl. Phys.* **36**, 205 (2006).

<sup>2</sup>R. Brayner, A. Coute, J. Livage, C. Perrette, and C. Sicard, *Anal. Bioanal. Chem.* **401**, 581 (2011).



- <sup>3</sup>E. Michelini and A. Roda, *Anal. Bioanal. Chem.* **402**, 1785 (2012).
- <sup>4</sup>A. Ramos, H. Morgan, N. G. Green, and A. Castellanos, *J. Phys. D: Appl. Phys.* **31**, 2338 (1998).
- <sup>5</sup>I.-F. Cheng, H.-C. Chang, D. Hou, and H.-C. Chang, *Biomicrofluidics* **1**, 021503 (2007).
- <sup>6</sup>R. Pethig, *Biomicrofluidics* **4**, 022811 (2010).
- <sup>7</sup>K. Khoshmanesh, S. Nahavandi, S. Baratchi, A. Mitchell, and K. Kalantar-Zadeh, *Biosens. Bioelectron.* **26**, 1800 (2011).
- <sup>8</sup>S. Gupta, R. G. Alargova, P. K. Kilpatrick, and O. D. Velev, *Langmuir* **26**, 3441 (2010).
- <sup>9</sup>S. O. Lumsdon, E. W. Kaler, and O. D. Velev, *Langmuir* **20**, 2108 (2004).
- <sup>10</sup>J. Kadaksham, P. Singh, and N. Aubry, *Electrophoresis* **26**, 3738 (2005).
- <sup>11</sup>V. Giner, M. Sancho, R. S. Lee, G. Martinez, and R. Pethig, *J. Phys. D: Appl. Phys.* **32**, 1182 (1999).
- <sup>12</sup>Y. Hubner, K. F. Hoettges, and M. P. Hughes, *J. Environ. Monit.* **5**, 861 (2003).
- <sup>13</sup>D. M. Graham, M. A. Messerli, and R. Pethig, *Biotechniques* **52**, 39 (2012).
- <sup>14</sup>N. M. Jesús-Pérez and B. H. Lapirozco-Encinas, *Electrophoresis* **32**, 2331 (2011).
- <sup>15</sup>H. O. Fatoyinbo, M. P. Hughes, S. P. Martin, P. Pashby, and F. H. Labeed, *J. Environ. Monit.* **9**, 87 (2007).
- <sup>16</sup>Z. R. Gagnon, *Electrophoresis* **32**, 2466 (2011).
- <sup>17</sup>F. H. Fernandez-Morales, J. E. Duarte, and J. Samitier-Marti, *An. Acad. Bras. Cienc.* **80**, 627 (2008).
- <sup>18</sup>K. Khoshmanesh, S. Baratchi, F. J. Tovar-Lopez, S. Nahavandi, D. Wlodkowic, A. Mitchell, and K. Kalantar-Zadeh, *Microfluid. Nanofluid.* **12**, 597 (2012).
- <sup>19</sup>K. Zhu, A. S. Kaprelyants, E. G. Salina, and G. H. Markx, *Biomicrofluidics* **4**, 022809 (2010).
- <sup>20</sup>H. Narayanan Unni, D. Hartono, L. Yue Lanry Yung, M. Mah-Lee Ng, H. Pueh Lee, B. Cheong Khoo, and K. M. Lim, *Biomicrofluidics* **6**, 12805 (2012).
- <sup>21</sup>S. Gupta, R. G. Alargova, P. K. Kilpatrick, and O. D. Velev, *Soft Matter* **4**, 726 (2008).
- <sup>22</sup>G. H. Markx, Y. Huang, X. F. Zhou, and R. Pethig, *Microbiology* **140**, 585 (1994).
- <sup>23</sup>N. Flores-Rodriguez and G. H. Markx, *J. Phys. D: Appl. Phys.* **37**, 353 (2004).
- <sup>24</sup>H. Morgan, M. P. Hughes, and N. G. Green, *Biophys. J.* **77**, 516 (1999).
- <sup>25</sup>J. Suehiro, R. Hamada, D. Noutomi, M. Shutou, and M. Hara, *J. Electroanal. Chem.* **57**, 157 (2003).
- <sup>26</sup>K. H. Bhatt and O. D. Velev, *Langmuir* **20**, 467 (2004).
- <sup>27</sup>M. Z. Bazant and T. M. Squires, *Curr. Opin. Colloid Interface Sci.* **15**, 203 (2010).
- <sup>28</sup>E. M. Melvin, B. R. Moore, K. H. Gilchrist, S. Grego, and O. D. Velev, *Biomicrofluidics* **5**, 034113 (2011).
- <sup>29</sup>K. H. Bhatt, S. Grego, and O. D. Velev, *Langmuir* **21**, 6603 (2005).
- <sup>30</sup>R. Krishnan, B. D. Sullivan, R. L. Mifflin, S. C. Esener, and M. J. Heller, *Electrophoresis* **29**, 1765 (2008).
- <sup>31</sup>See supplementary material at <http://dx.doi.org/10.1063/1.4801870> for polarizability calculations using multishell model.
- <sup>32</sup>O. D. Velev and K. H. Bhatt, *Soft Matter* **2**, 738 (2006).
- <sup>33</sup>J. Kim, J. L. Anderson, S. Garoff, and P. J. Sides, *Langmuir* **18**, 5387 (2002).
- <sup>34</sup>C. Lamelas, K. J. Wilkinson, and V. I. Slaveykova, *Environ. Sci. Technol.* **39**, 6109 (2005).
- <sup>35</sup>K. Knauer and J. Buffle, *J. Phycol.* **37**, 47 (2001).
- <sup>36</sup>D. S. Gray, J. L. Tan, J. Voldman, and C. S. Chen, *Biosens. Bioelectron.* **19**, 1765 (2004).